STUDY OF BASIC RF BREAKDOWN PHENOMENA IN HIGH GRADIENT VACUUM STRUCTURES *

V. A. Dolgashev, S. G. Tantawi, SLAC, Menlo Park, CA, 94025, USA
Y. Higashi, KEK, Tsukuba, Japan
B. Spataro, INFN-LNF, Frascati, Italy

Abstract

We present the results of R&D aimed at exploring the basic physics of RF breakdown phenomena in high vacuum structures. We performed an extensive experimental survey of materials for RF magnetic field induced metal fatigue. To do this, we designed a cavity operating at a TE01m-like mode which focuses RF magnetic field on the flat sample surface. We tested more than 20 samples of materials including single crystal copper and copper alloys. With these results in hand, we constructed standing wave cavities of different geometries and materials to conduct RF-breakdown experiments. To study a broad range of materials and surfaces, we explored different structure-joining techniques, including those which allow us to avoid high temperature brazing. Using structures of different geometries, we examined the effect of the mixture of surface electric and magnetic fields on breakdown behavior. The experiments were done at 11.4 GHz.

INTRODUCTION

Accelerating gradient is one of the crucial parameters affecting the design, construction and cost of the next-generation linear accelerators. RF breakdown is the major obstacle to higher gradient. RF breakdown limits the working power and produces irreversible surface damage in high power rf components and rf sources.

The accelerating gradient of the long-lived SLAC S-band linac is 20 MV/m. During development of the Next Linear Collider (NLC)/Global Linear Collider (GLC), an X-band test accelerator was built that operated at 65 MV/m unloaded gradient [1, 2]. The CERN based linear collider design CLIC requires 100 MV/m loaded gradient at 12 GHz in accelerating structures with heavy wakefield damping [3]. Future accelerators may need even higher gradients for compact synchrotron light sources or inverse Compton scattering gamma ray sources [4].

A major investment in the study of rf breakdown in X-band accelerating structures and high power rf components was made during the NLC/GLC development [5, 6, 7]. Currently this work is continued by the US High Gradient Collaboration together with CERN, KEK, and INFN-LNF Frascati [8, 9]. Although this study advanced our understanding of the subject, many questions about the physics of rf breakdown remain unanswered. Up to now, there is no theory or simulation method that can predict breakdown performance of accelerating structures or high power rf components during their technical design. Here we discuss the results of experiments that study the basic physics of rf breakdown in short standing-wave (SW), traveling-wave (TW) accelerating structures, and experiments that explore the effects of the high rf magnetic fields on a metal surface.

Breakdown rate

During the last decade of rf breakdown studies, we found that for a given accelerating structure and a fixed rf pulse shape, the probability of an rf breakdown (number of breakdowns per total number of rf pulses) is a value slowly varying with time. A typical example of accumulated breakdowns *vs.* time for a single-cell SW structure is shown in Fig. 1a). Here we show only the so called *first breakdowns* in a cluster (see Ref. [10]). We speculate that the first-breakdowns reflect the characteristics of the breakdown trigger.

The accumulated breakdowns closely follow a linear fit, which is remarkable for such a complex phenomena. The histogram of time interval between subsequent breakdowns is shown on Fig. 1b). We found that the curve follows exponential distribution, which means that the breakdown events occur continuously and independently at a constant average rate.

One of the results of the high power test of an accelerating structure is the breakdown rate map, or dependence of the breakdown rate on rf pulse shape [11]. Utilizing the breakdown rate maps to characterize the structures allows us to avoid the use of ambiguous terms such as “breakdown limit”.

Reproducibility

Reproducibility of the breakdown rate maps is one of the main results of dozens of tests of the X-band TW and SW structures. We found that for structures of the same geometry and material, the breakdown maps are remarkably reproducible. This was verified for structures made by different laboratories and for a range of initial surface conditions.

There are several practical consequences of this reproducibility. First, the breakdown performance data could be interpolated to new structure geometries, meanwhile the extrapolation of the data beyond explored parameter space is often invalid. Second, to be able to predict the breakdown rate, a physical model of the breakdown performance should have the structure geometry and the material properties as the main (and maybe the only) input parameters.

PULSED HEATING EXPERIMENTS

Early high power tests of accelerating structures and waveguides showed that the rf magnetic fields and cyclic thermal stresses, produced by rf pulsed heating, influence

* This work is supported by the US department of energy under contract DE-AC02-76-SFO0515.

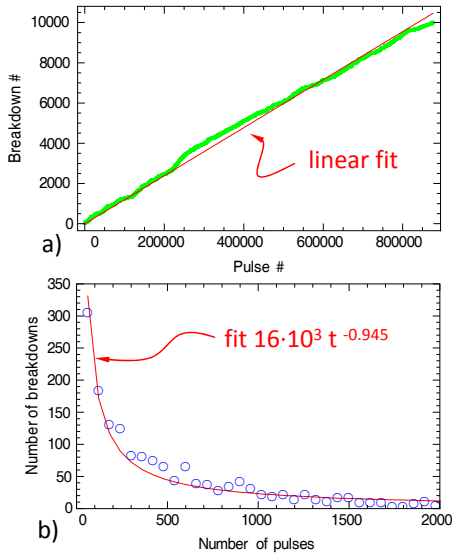

Figure 1: Typical breakdown data from one experiment with constant rf pulse shape and rf power: a) number of accumulated breakdowns *vs.* pulse number, b) histogram of number of pulses between consequent breakdowns with fit to exponential distribution.

the behavior of the rf breakdowns [12, 13]. An experimental study was conducted aimed at determining the potential of different materials for tolerating cyclic thermal fatigue due to rf magnetic fields [14, 15]. Here we briefly outline some results of this study.

On Fig. 2a) we show scanning-electron microscope image of a soft copper sample. The pulsed heating creates a ring of damage on the metal surface. The peak temperature rise in the middle of the ring is $\sim 110°$C. One can see that the first detectable changes in the copper surface starts on the grain boundaries at a peak pulse heating temperature of about $50°$C, and that the damage is strongly influenced by the grain orientation: some grains are not damaged even at the location where the temperature is maximum. On Fig. 2b) we show a typical iris of a short SW structure after the high power test. The damage from the rf breakdowns increases toward the iris aperture, and the typical pulsed heating damage is seen in the region with high rf magnetic fields.

Another major result of these experiments is that hardened copper and hardened copper alloys show significantly less pulse heating damage than soft, heat treated metals. With these results in hand, we constructed SW structures from both soft and hardened copper and copper alloys. Some result of these tests are reported below.

GEOMETRIC EFFECTS

Standing-Wave Structures

To understand geometric effects on the breakdown rates at a given gradient we conducted a series of experiments with short standing wave structures of different geometries [16, 8]. Four different types of structures were constructed. Three of them have elliptically shaped irises and different iris diameters. The iris shape of these structures is elliptical to reduce electrical field on the iris tips by decreasing local curvature at the high electric field region. We made the fourth structure with round iris in order to intentionally increase peak surface electric field while keeping the same peak surface magnetic field. The structure shapes are shown in Fig. 3 and the properties of the middle, high field cell of these structures at a gradient of 100 MV/m are summarized in Table 1.

The breakdown rate was measured for these structures and the results are shown in Fig. 4 a), b), and c). One

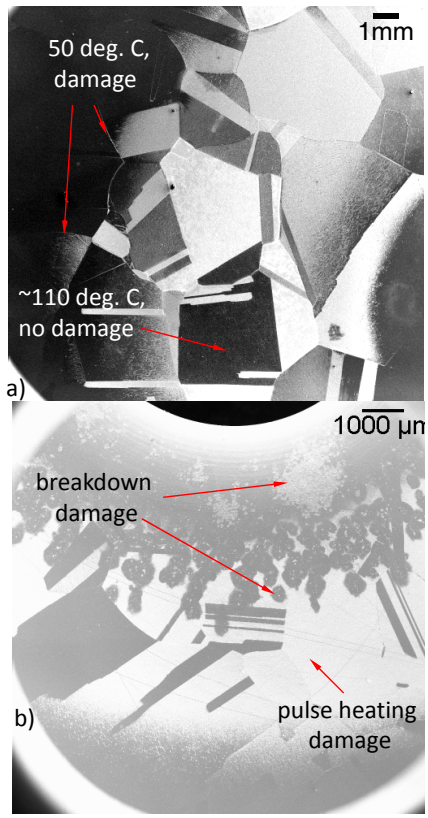

Figure 2: Scanning Electron Microscope pictures of the pulse heating damage on a) flat sample and b) iris of SW structure. Peak pulsed temperature was $\sim 110°$C on the sample and $\sim 80°$C on the iris.

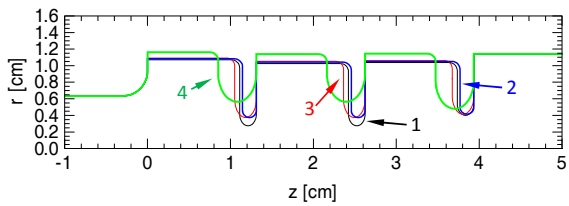

Figure 3: Geometries of 4 SW structures: 1) $a/\lambda = 0.105$ (elliptical iris); 2) $a/\lambda = 0.143$ (round iris); 3) $a/\lambda = 0.143$ (elliptical iris); 4) $a/\lambda = 0.215$ (elliptical iris). RF power is fed into the structure from the right. A cutoff waveguide is on the left.

Table 1: Parameters of periodic π phase advance SW structures. The parameters are normalized to 100 MV/m accelerating gradient. Frequency is 11.424 GHz. Cell length is 1.312 mm.

Structure name	A2.75-T2.0-Cu	A3.75-T1.66-Cu	A3.75-T2.6-Cu	A5.65-T4.6-Cu
Stored energy [J]	0.153	0.189	0.189	0.298
Q-value [10^3]	8.59	8.82	8.56	8.38
Shunt impedance [MOhm/m]	102.891	85.189	82.598	51.359
H_{max} [MA/m]	0.290	0.314	0.325	0.418
E_{max} [MV/m]	203.1	266	202.9	211.4
Losses in a cell [MW]	1.275	1.54	1.588	2.554
a [mm]	2.75	3.75	3.75	5.65
a/λ	0.105	0.143	0.143	0.215
$H_{max}Z_0/E_{acc}$	1.093	1.181	1.224	1.575
t [mm]	2.0	1.66	2.6	4.6
Iris ellipticity	1.4	1.0	1.7	1.5

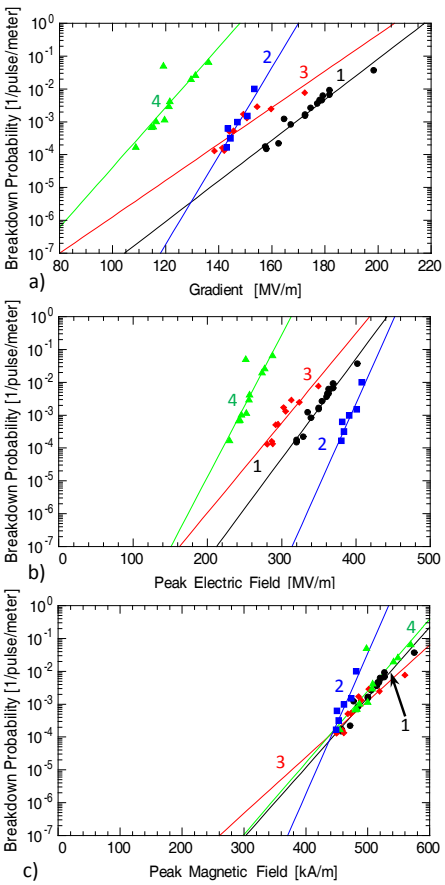

Figure 4: Comparison between four different structures with different iris shapes. The data is for a shaped rf pulse with $\sim$ 170 ns charging time and 200 ns flat part for structures 1, 2, 3 and 150 ns flat part for structure 4.

can see from the first two figures that the data does not correlate at all with either the accelerating gradient or the surface electric field. For the same breakdown probability one finds that the peak surface electric field varies by a factor of 1.6. Two accelerating structures with different peak electric fields, one operating at 250 MV/m surface field and the other operating at 400 MV/m have the same breakdown rate. The picture is quite different if one looks at Fig. 4c). Most of the data correlates well with peak magnetic field. This result is even more obvious when we compare structures (2) and (3). Both structures have the same iris diameter but different iris shape. In the structure (2) with a round iris, the ratio between peak surface electric field and the gradient is 2.66 and in (3) with elliptical iris it is 2.03. At the breakdown rate 10^{-4}/pulse/m both structures have the same gradient and peak magnetic field while peak surface electric field is 290 MV/m for the structure with the elliptical iris and 390 MV/m for the structure with the round iris.

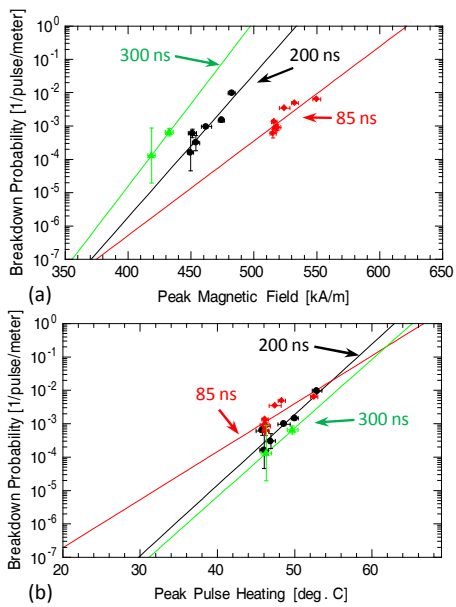

Figure 5: Breakdown rates as a function of peak magnetic field(a) and as a function of the peak pulsed heating during the pulse(b). Data is for shaped rf pulse with $\sim$ 170 ns charging time.

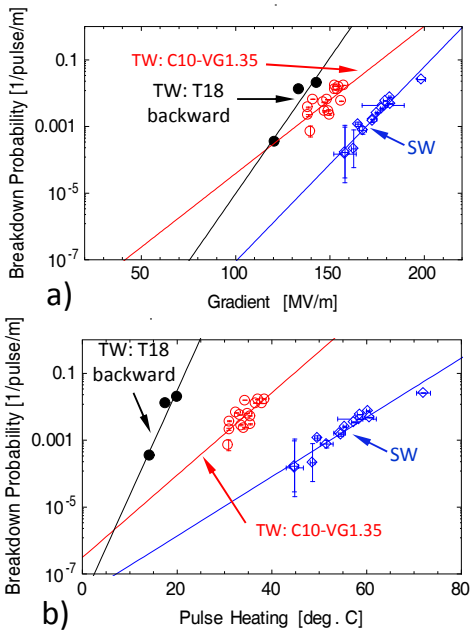

Figure 6: Comparison of two TW structures and one SW structure with $\sim$ 3 mm aperture. Breakdown rate *vs.* a) gradient and b) peak pulse surface heating.

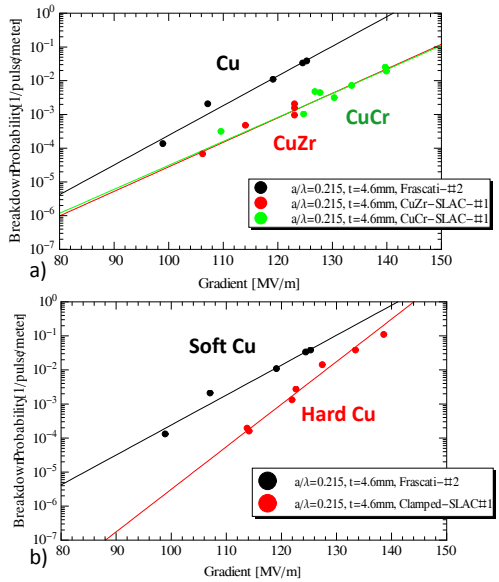

Figure 7: Comparison of SW structures made of copper and different copper alloys. Breakdown rate *vs.* gradient for brazed structures, and b) soft (brazed) and hard (clamped) copper. The data is for a shaped rf pulse with $\sim$ 170 ns charging time and 150 ns flat part.

Breakdown probability varies with pulse duration as well as peak fields. Fig. 5 shows that the data would correlate better if one took the pulsed heating as figure of merit. The peak pulsed heating is proportional to the square of the magnetic field; see [17]. Indeed, the physics behind this is still an open problem. Further, pulsed heating is just a figure of merit that combines the square of the magnetic field and roughly the square root of the pulse length. Certainly a theory that explains the origin of this experimental data is now needed.

Traveling Wave vs. Standing Wave Structures

We found that the breakdown rate is similar for different geometries of short standing wave structures at the same peak-pulse-heating temperature. This dependance is well reproduced for brazed copper structures of the disk loaded waveguide type. Typically, for these structures, the breakdown rate is below 10^{-4}/pulse/m rf for peak-pulse-heating temperatures below $40°$C.

Meanwhile, TW structures do not follow the same dependence on peak pulse heating temperature [18, 9]. A comparison of the breakdown data for two TW structures and one SW structure with similar aperture is shown in Fig.6. In all three structures, the breakdowns occured in one cell. For the same gradient, both TW structures have similar breakdown rates which is more than 10 times higher than the rate in the SW structure (see Fig.6a). For the same breakdown rate, the peak pulse heating in TW structures is about half of that in the SW structure (see Fig.6b)).

The SW structures have very low breakdown rate at pulse heating temperatures of about $40°$C (see Fig. 5b) and Fig. 6b)). This temperature is very close to the $\sim$ $50°$C where we detect first changes on the grain boundaries of samples in the pulsed heating experiments. When TW structures are run at the same breakdown rate as SW structures, the peak pulse heating temperature is half of that in the SW structures. Therefore, we speculate that it is unlikely for the breakdown trigger mechanism in TW structures to be directly related to pulse heating induced stresses on unperturbed metal surface.

NEW MATERIALS

We conducted tests of SW structures made of soft-copper alloys (CuAg, CuCr, CuZr) and hard-copper and hard-copper alloys (CuAg, CuZr). The results of these tests are reported in Ref. [8]. Here we show the results for the soft copper alloys and hard copper.

The structures made of soft-copper and soft-copper alloys show somewhat lower breakdown rate at the same gradient as shown on Fig. 7a). As in soft cooper structures, the breakdown rate in soft copper alloy structures is highly correlated with peak pulse surface heating temperature.

High power RF tests of the hard-copper structures showed some improvement over soft copper but not as dramatically as we expected based on the tests of the pulse heating samples (see Fig. 7b)). Unlike for the soft-Cu structures, we did not observe typical pulsed heating damage in the hard-Cu structures, although their breakdown rate correlated similarly with the peak pulse heating temperature.

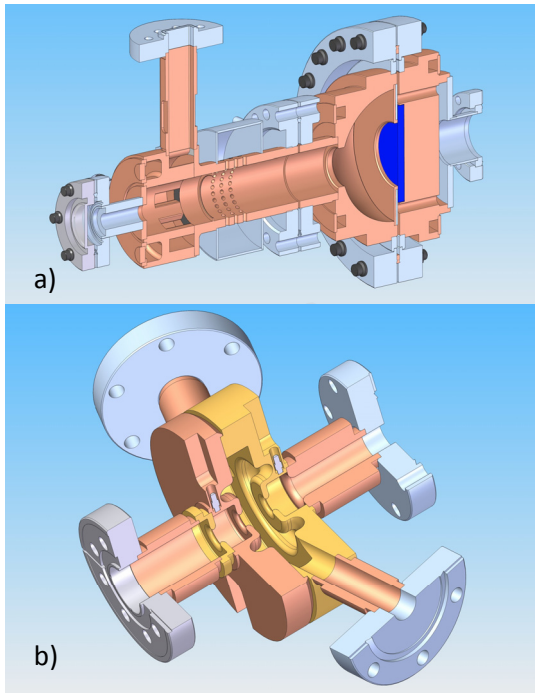

Figure 8: New setups for in-situ microscopic observation of the metal surfaces: a) cavity-mode-convertor assembly with a view-port for studies of pulsed heating damage, b) SW structure with two view ports for rf breakdown experiments.

FUTURE WORK

To obtain information about rf breakdowns, the experiments described in this paper relied on measurements of rf signals and post-test inspection of the cut apart structures. We plan to start new tests that employ in-situ microscopic observation of the metal surface. We have designed and manufactured a new cavity to study pulsed heating. The cavity is shown on Fig. 8a). It has an increased coupling iris and a window that allows observation of the metal surface with a long-focus length microscope or an infrared camera.

The second cavity; a short SW accelerating structure, is shown on Fig. 8b). The cavity has two view ports to watch the regions of both high electric and high magnetic fields [19]. This cavity is being manufactured at SLAC.

SUMMARY

We have presented the recent results of the study of rf breakdown in high gradient vacuum structures. In this work we used short SW and TW structures, and a cavity that focuses rf magnetic field on the surface of a metal sample. We found that the final breakdown rate dependence on the rf pulse shape and power is remarkably reproducible for different structures of the same geometry and material. For standing wave structures, the breakdown rate has strong dependence on the peak surface magnetic field and weaker dependence on the peak surface electric field. The traveling wave structures of the same aperture as standing wave structures have about 20-30% lower gradient and about half the peak pulse heating temperature for the same breakdown rate. We found that in the soft copper the pulsed heating damage starts at about 50°C at the grain boundaries. We tested SW structures made of hard copper and both soft and hard copper alloys. We are building new cavities that allow in-situ microscopic observation of the changes on metal surface due to rf pulsed heating and rf breakdowns.

ACKNOWLEDGMENTS

This work was started within the scope of the NLC/GLC project and is currently continued by US High Gradient collaboration together with KEK, CERN and INFN Frascati. We especially thank A. Yeremian, J. Lewandowski, J. Wang, C. Adolphsen, F. Wang, E. Jongewaard, C. Pearson, A. Vlieks, J. Eichner, D. Martin, C. Yoneda, L. Laurent, A. Haase, R. Talley, J. Zelinski, J. Van Pelt, R. Kirby, Z. Li, S. Weathersby of SLAC; T. Higo of KEK; W. Wuensch of CERN.

REFERENCES

[1] S. Doebert *et al.*, in *Proc. of IEEE PAC 2005, Knoxville, Tennessee*, pp. 372–374, 2005. SLAC-PUB-11207.

[2] J. W. Wang, *High Energy Phys. Nucl. Phys.*, vol. 30, p. 11, 2006. SLAC-PUB-12293.

[3] G. Guignard, "The CLIC Study Team," 2000. CERN Report No. CERN 2000-008.

[4] F. V. Hartemann and F. Albert, in *LLNL Technical Report, LLNL-TR-416320*, 2009.

[5] J. Wang and T. Higo, *ICFA Beam Dyn. Newslett.*, vol. 32, p. 27, 2003.

[6] C. Adolphsen, in *Proc. of IEEE PAC 2003, Portland, Oregon*, pp. 668–672, 2003.

[7] V. A. Dolgashev *et al.*, in *Proc. of IEEE PAC 2003, Portland, Oregon*, pp. 1264–1266, 2003.

[8] V. Dolgashev *et al.*, in *Proc. of IPAC 2010, Kyoto, Japan*, pp. 3810–3812, 2010.

[9] T. Higo *et al.*, in *Proc. of IPAC 2010, Kyoto, Japan*, pp. 3702–3704, 2010.

[10] V. Dolgashev *et al.*, in *Proc. of IEEE PAC 2005, Knoxville, Tennessee*, pp. 595–599, 2005. SLAC-PUB-11707.

[11] V. Dolgashev *et al.*, in *Proc. of IEEE PAC 2007, Albuquerque, New Mexico*, pp. 2430–2432, 2007. SLAC-PUB-12956.

[12] V. A. Dolgashev and S. G. Tantawi, in *Proc. of EPAC 2002, Paris, France*, pp. 2139–2141, 2002.

[13] V. A. Dolgashev, in *Proc. of IEEE PAC 2003, Portland, Oregon*, pp. 1267–1269, 2003. SLAC-PUB-10123.

[14] L. Laurent *et al.*, MOP076, LINAC10, 12-17 September 2010, Tsukuba, Japan.

[15] S. Heikkinen, *Study of High Power RF Induced Thermal Fatigue in the High Gradient Accelerating Structures*. PhD thesis, Helsinki University of Technology, Finland, 2008.

[16] V. Dolgashev *et al.*, in *Proc. of EPAC 2008, Genoa, Italy*, pp. 742–744, 2008.

[17] D. P. Pritzkau and R. H. Siemann, *Phys. Rev. ST Accel. Beams*, vol. 5, p. 112002, Nov 2002.

[18] R. Zennaro *et al.*, in *Proc. of EPAC 2008, Genoa, Italy*, pp. 533–535, 2008.

[19] A. Yeremian *et al.*, in *Proc. of IPAC 2010, Kyoto, Japan*, pp. 3822–3824, 2010.